Food Chemistry 170 (2015) 226–233

Contents lists available at ScienceDirect

Food Chemistry

journal homepage: www.elsevier.com/locate/foodchem

Copigmentation of malvidin-3-*O*-glucoside with five hydroxybenzoic acids in red wine model solutions: Experimental and theoretical investigations

Bo Zhang [a], Rui Liu [a], Fei He [a], Pan-Pan Zhou [b], Chang-Qing Duan [a,*]

[a] Center for Viticulture and Enology, College of Food Science & Nutritional Engineering, China Agricultural University, Beijing 100083, China
[b] College of Chemistry and Chemical Engineering, Lanzhou University, Lanzhou 730000, China

ARTICLE INFO

Article history:
Received 6 June 2014
Received in revised form 6 August 2014
Accepted 7 August 2014
Available online 18 August 2014

Keywords:
Copigmentation
Anthocyanin
Hydroxybenzoic acid
Thermodynamic parameters
Theoretical calculations

ABSTRACT

In the present research, the copigmentations of malvidin-3-*O*-glucoside with five hydroxybenzoic cofactors (*p*-hydroxybenzoic acid, protocatechuic acid, gallic acid, vanillic acid, and syringic acid) were investigated. The influence of the concentration of these cofactors and the reaction temperature was examined. The equilibrium constant (K), stoichiometric ratio (n) and the thermodynamic parameters ($\Delta G°$, $\Delta H°$, $\Delta S°$) related to the copigmentation were also reported here. Theoretical calculations were performed to identify the relative arrangement between the pigment and cofactors in the copigmentation complexes. Besides, the comparison of the relative binding free energies ($\Delta\Delta G_{binding}$) derived from the theoretical calculations and experimental data were made, and the binding strength of these copigmentation complexes was discussed with the interaction energies (ΔE). AIM analysis was also used to explore the main driving forces contributing to the copigmentation. In the comparison of the five studied cofactors, syringic acid had a stronger copigmentation effect than the other four phenolic acids investigated.

1. Introduction

Anthocyanins have attracted great interests in the past several decades due to their important roles as natural pigments that were responsible for the colour of many beverages, especially in red wine, as well as their numerous health promoting benefits (He & Giusti, 2010; Qin et al., 2009; Sancho & Pastore, 2012; Vauzour, Rodriguez-Mateos, Corona, Oruna-Concha, & Spencer, 2010). The colour exhibited by anthocyanins is strongly dependent on the pH of their aqueous solution. At a low pH (<2.0), anthocyanins' red colour appears because of their predominant flavylium cation. With the increasing of pH, the other forms of anthocyanins (hemiketal, chalcones, and quinonoidal bases) were generated in the equilibrium (Raymond Brouillard & Delaporte, 1977). When the pH is in the range of 2.0–4.0, the anthocyanins exist as colourless hemiketals (>70%) in tautomerism equilibrium with pale yellow *cis*-chalcone and *trans*-chalcone forms. And at higher pH values, they are present as quinoidal bases (neutral and anionic) (Brouillard, Mazza, Saad, Albrecht-Gary, & Cheminat, 1989). Thus, at the normal pH of wine (3.2–4.0) most of the anthocyanins are expected to exist as colourless hemiacetals in equilibrium with other forms. However, in nature, coloured flavylium cation and quinonoidal forms of anthocyanins are predominant in red wine, which suggests that some stabilizing mechanisms may exist and improve chemical and colourimetric stability of anthocyanins. Many studies have suggested that the enhanced colour of the solutions could be ascribed to the intermolecular interactions between the flavylium cation of anthocyanin and the cofactor in copigmentation, which would stabilize the flavylium cation chromophore (benzopyrylium) and block its interactions with water molecules, thus keeping the colour without loss (Goto, 1987; Santos-Buelga & de Freitas, 2009).

The copigmentation results in an increase of absorbance in the visible range (hyperchromic shift) and a positive shift of the wavelength of the maximum absorbance (bathochromic shift), making the changes of colour tendency and intensity detectable (Malaj, De Simone, Quartarolo, & Russo, 2013; Teixeira et al., 2013). Besides, such as the ionic strength, pH, solvent, temperature, the presence of metal salts (Asen, Stewart, & Norris, 1972; Raymond Brouillard & Dangles, 1994; Mistry, Cai, Lilley, & Haslam, 1991), the molecular structures of anthocyanins and cofactors are also important for the copigmentation (Sousa et al., 2014). In addition, as a special case, another copigmentation mechanism caused by anthocyanins themselves when their concentrations were higher than 1 mM was also reported, which was named as self-association (Boulton, 2001). Self-associations of anthocyanins were observed

* Corresponding author. Tel./fax: +86 10 62737136.
E-mail address: chqduan@cau.edu.cn (C.-Q. Duan).

http://dx.doi.org/10.1016/j.foodchem.2014.08.026
0308-8146/

to take place during wine aging and it was assumed that they might partially contribute to the colour of aged wines (Rein, 2005). Because the copigmentation is essentially of noncovalent interactions (e.g., hydrogen bond, van der Waals interaction), the proton donors, acceptors, and the aromatic rings of them are also crucial for the formations of these interactions. For instance in some previous reports, the flavonols (quercetin and rutin) exhibited a strong copigmentation effect, while the flavan-3-ols (epicatechin and catechin) were relatively weaker (Lambert, Asenstorfer, Williamson, Iland, & Jones, 2011). The phenolic acids, like sinapic acid and ferulic acid, had strong copigmentation with colour enhancement and bathochromic shift (Markovic, Petranovic, & Baranac, 2000; Sun, Cao, Bai, Liao, & Hu, 2010), and some of them were evaluated as external polyphenolic cofactors which could enhance and stabilize anthocyanins' colour in red wine (Aleixandre-Tudó et al., 2013; Bloomfield, Heatherbell, & Pour Nikfardjam, 2003; Schwarz, Picazo-Bacete, Winterhalter, & Hermosín-Gutiérrez, 2005). These compounds mentioned above normally contain one or more phenolic rings, and the π–π interaction between the aromatic rings of these phenols and anthocyanins served as a driving force of the copigmentation. Additionally, the hydroxyl or carbonyl *O* group linking to the phenolic ring might also interact with anthocyanin to form hydrogen bond or charge transfer interactions. Obviously, the cofactors containing phenolic ring and hydroxyl or carbonyl *O* group would be implicated in the intermolecular interactions, leading to a strong copigmentation with anthocyanin.

Hydroxybenzoic acids are characterized by their C_6–C_1 skeletons, which are one class of the most representative phenolic acids found in both of grapes and wines. Because of their significant roles in enhancing and stabilizing red wine colour, great interests were focused on their abilities as cofactors (Malaj et al., 2013). Therefore, to understand the detailed abilities of different hydroxybenzoic acids in red wine as cofactors of anthocyanin are quite important. In this research, the intermolecular copigmentation between the anthocyanin, malvidin-3-*O*-glucoside (M3OG), and five different hydroxybenzoic cofactors [*p*-hydroxybenzoic acid (*p*HA), protocatechuic acid (PA), gallic acid (GA), vanillic acid (VA), and syringic acid (SA)] (Fig. S1, Supplementary Material) were evaluated by determination of their respective spectral and thermodynamic parameters. Meanwhile, the effects of the cofactor's concentration and temperature in reactions were examined, and the interaction strengths of these copigmentation complexes were also compared and discussed with theoretical calculations.

2. Materials and methods

2.1. Materials

The anthocyanin, M3OG was purchased from Phyto Lab GmbH & Co. (Vestenbergsgreuth, Germany), while the chemicals of *p*HA, PA, GA, VA, and SA were supplied by Sigma–Aldrich (St. Louis, MO, USA). Deionised water (<18 MW resistance) was obtained from a Milli-Q Element water purification system (Millipore, Bedford, MA, USA). All the other chemicals were obtained from Sigma–Aldrich, unless noted specially.

2.2. Preparation of model wine solutions

The model wine solutions were prepared as following: tartaric acid (5 g/L) with 12% ethanol at pH 3.6, and the ionic strength was adjusted to 0.2 M by the addition of NaCl (Nonier Bourden et al., 2008). For assessing the effect of molar ratio on the copigmentation, five cofactors' solutions (*p*HA/M3OG, PA/M3OG, GA/M3OG, VA/M3OG, SA/M3OG) were prepared by mixing 0.20 mM anthocyanin with an aliquot of cofactor solution to obtain the pigment/cofactor molar ratio of 1:0, 1:1, 1:10, 1:20, 1:40, 1:80, 1:100 at 20 °C. The influence of temperature was evaluated with molar ratio of 1:40 at 10, 15, 20, 25, and 30 °C. All of these solutions were prepared in triplicate, and they were stored in darkness to equilibrate for 30 min. Then their absorption spectra were recorded by using a UV–Visible spectrophotometer (Shimadzu UV-2450, Shimadzu Corporation, Kyoto, Japan). Visible absorption spectra (400–700 nm) of solutions were recorded periodically at constant the interval ($\Delta\lambda$ = 1 nm), by using 1 cm path length glass cells. The experiments were based on the reported method (Brouillard et al., 1989) with some modifications.

2.3. Thermodynamic data determination

The values of equilibrium constant (K), Gibbs free energy (ΔG°), enthalpy change (ΔH°), and entropy change (ΔS°) of the copigmentation reaction were determined by the Eqs. (1)–(4) (Brouillard et al., 1989; Lambert et al., 2011).

$$\ln\left(\frac{A-A_0}{A_0}\right) = \ln K + n\ln[\mathrm{CP}]_0 \quad (1)$$

$$\Delta G^0 = -RT \times \ln K \quad (2)$$

$$\Delta G^0 = \Delta H^0 - T\Delta S^0 \quad (3)$$

$$\ln\left(\frac{A-A_0}{A_0}\right) = \frac{\Delta H}{RT} + \frac{\Delta S^0}{\mathrm{R}} + n\ln[\mathrm{CP}]_0 \quad (4)$$

Among them, A_0 was the maximum visible absorbance at λ = 520 nm for M3OG in the absence of the cofactors, and A was the absorbance at λ_{520} of M3OG in the presence of the cofactors. K was the equilibrium constant for the reaction of the copigmentation, and it was expressed as $[\mathrm{AH(CP)}_n^+]/([\mathrm{AH}^+][\mathrm{CP}]^n)$ (Malaj et al., 2013). And, n was the stoichiometric ratio between the anthocyanin and the cofactor. $[\mathrm{CP}]_0$ represented the concentration of cofactor added to the anthocyanin solution, R was the gas constant (8.314 J/mol K), and T was the temperature in Kelvin.

2.4. Molecular dynamic simulations

To evaluate the interactions between the pigment (M3OG) and cofactors (*p*HA, PA, GA, VA and SA), the starting geometries of these molecules were optimized by using Hyperchem 7.0 package (Hypercube Inc., USA) via molecular mechanics (MM) force field. Then five interaction models for the pigment and cofactors were constructed, and the geometries of these complexes were also optimized via MM force field. The geometries of molecules and complexes were further optimized by using the M062X functional (Zhao & Truhlar, 2006, 2008) with the 6–31G (d, p) basis set, because of the accuracy of the M062X functional in treating noncovalent interactions and the less computational cost, which were implemented in the Gaussian 09 package (Frisch et al., 2009). The integral equation formalism polarizable continuum model (IEFPCM) method was also used to consider the solvent effect.

The binding Gibbs free energy ($\Delta G_{\mathrm{binding}}$) and interaction energy (ΔE) for the copigmentation complex were calculated via the following equations:

$$\Delta G_{\mathrm{binding}} = G_{\mathrm{complex}} - G_{\mathrm{copi}} - G_{\mathrm{pi}} \quad (5)$$

$$\Delta E = E_{\mathrm{complex}} - E_{\mathrm{copi}} - E_{\mathrm{pi}} \quad (6)$$

For Eq. (5), G_{complex}, G_{copi}, and G_{pi} were the Gibbs free energies of the copigmentation complex, the cofactor, and the pigment, respectively. The similar binding modes were observed due to

the similar structures of the cofactors, and therefore, the relative binding free energies ($\Delta\Delta G_{binding}$) were calculated relative to the most stable copigmentation complex. For Eq. (6), $E_{complex}$, E_{copi}, and E_{pi} denoted the total energy of the copigmentation complex and the energies of the cofactor and pigment, respectively.

3. Results and discussion

3.1. Spectral characteristics of M3OG with cofactors

The ability of the phenolic acid to act as cofactors was surveyed in 12% ethanol–water solution at pH 3.6. To avoid the self-association effect, a suitable concentration of M3OG (2.0×10^{-4} M) was used. Generally, there was no considerable absorbance of the phenolic acids in the visible part of the spectrum (Kelebek, Selli, Canbas, & Cabaroglu, 2009). Thus, the increase of the absorbance reflected a strong interaction between the pigment and cofactor, and such variation can be measured by the values of hyperchromic and bathochromic shifts in the maximum absorbance (Brouillard et al., 1989), in which their values were reported as $(A - A_0)/A_0$ and $\Delta\lambda_{max} = \lambda_{max} - \lambda_{520}$, respectively.

As shown in Fig. 1(a–e), continuous increases of absorbance with the increasing concentrations of the cofactors in the solutions were observed, indicating strong intermolecular interactions between the pigments and the cofactors, which was responsible for the colouration of these solutions. The relatively strongest copigmentations for the complexes of M3OG and the five phenolic acids (*p*HA, PA, GA, VA and SA) were observed at the 1:100 M ratio, showing that the higher concentrations of the cofactors usually appeared stronger effects in the copigmentations. Among these cofactors, the greatest magnitude of copigmentation was induced by SA, exhibiting the greater hyperchromic shifts of 2.0–125.8% at the molar ratio from 1:1 to 1:100 (Table S1, Supplementary Material). Whereas copigmentations of the *p*HA and PA with M3OG were weaker, which represented the colour enhancements of 1.0–30.0% and 1.0–49.2%, respectively. The GA and VA were also relatively good cofactors, and their interactions with M3OG increased the visible absorption by 75.8% and 85.9% at the 1:100 M ratio, respectively. Besides the hyperchromic shift, the bathochromic shifts also increased with the increasing concentrations of cofactors in solution, as shown in Table S1. These results suggested that both the hyperchromic and bathochromic shifts were strongly influenced by the highest concentration of these cofactors.

$$AH^+ \leftrightarrow A + H^+ \quad (7)$$

$$AH^+ + H_2O \leftrightarrow (B + C_E) + H^+ \quad (8)$$

$$AH^+ + nCP \leftrightarrow AH(CP)_n^+ \quad (9)$$

The hyperchromic and bathochromic shifts could be ascribed to a displacement of the hydration equilibrium, which were illustrated by Eqs. 7–9. The formation of the complexes between colourless phenolic acids and the flavylium cations of malvidin-3-*O*-glucoside would lead to the equilibrium of the anthocyanins toward the formation of flavylium ions, which could enhanced the red colour intensities of the solutions. While another consequence associated with copigmentation was a bathochromic shift, which was an increase of the solution's λ_{max} (Schwarz et al., 2005; Álvarez, Aleixandre, García, Lizama, & Aleixandre-Tudó, 2008).

Among the five analyzed cofactors, the different hyperchromic and bathochromic shifts observed in Table S1 might be related to the substituent groups linked to the hydroxybenzoic acid molecules. Compared to *p*HA, PA and GA possessed more hydroxyl groups, so the larger hyperchromic and bathochromic shifts were observed for their copigmentations with M3OG. Because the methoxyl group had a larger size than the hydroxyl group, the copigmentation of VA or SA with M3OG resulted in the larger hyperchromic and bathochromic shifts. These findings might be caused by more hydrogen bonds formed between anthocyanins and the cofactors containing more hydroxyl or methoxyl groups (Malaj et al., 2013; Sun et al., 2010) and more lubricity (Rein, 2005). However, such mechanism still needed our further supports with the thermodynamic studies.

3.2. Thermodynamic data for the copigmentation

From the viewpoint of thermodynamics, the consequences raised from the interaction of anthocyanins with different cofactors could provide information on the energy changes of copigmentation and the inherent mechanism. The equilibrium constant (K) for the copigmentation reaction gave out the strength between the cofactor and the anthocyanin. In this study, $\ln K$ was the intercept of the plot of $\ln[(A - A_0)/A_0]$ *vs* $\ln[CP]_0$ (Fig. 1f). With regards to the different cofactors, the $\ln[(A - A_0)/A_0]$ *vs* $\ln[CP]_0$ plots displayed straight lines with good correlation coefficients ($R^2 > 0.95$). The values of equilibrium constants K determined by this method also followed the order of *p*HA/M3OG < PA/M3OG < GA/M3OG < VA/M3OG < SA/M3OG (Table 1). This was consistent with the tendency of bathochromic shift discussed above. The K values of VA/M3OG and SA/M3OG were similar to those in the previous work (Malaj et al., 2013). As suggested by Malaj et al. (2013), the K value was an important indicator of the strength of the association pigment-cofactor complex, so a large value meant a strong binding between them. It could be expected that the binding strengths for the copigmentation reactions were the same as the order of K values. Of course, these results should be related to the structural features because the cofactors with more hydroxyl or methoxyl groups might form more hydrogen bonds with M3OG to showing stronger interactions, which was agreed with some previous findings (Teixeira et al., 2013). The stoichiometric constant (n) determined by the plots of $\ln[(A - A_0)/A_0]$ *vs* $\ln[CP]_0$, describing the association between the cofactors and the researched anthocyanins. The copigmentation complexes showed that the n values approached to 1.0 (Table 1), indicating that the copigmentation between the pigment and the cofactor were as an 1:1 association, which were in agreement with some previous findings (Lambert et al., 2011; Malaj et al., 2013; Sun et al., 2010).

The variations of Gibbs free energies (ΔG°) were negative for all the copigmentation complexes (Table 1), suggesting that the processes of M3OG with the five cofactors (*p*HA, PA, GA, VA and SA) were spontaneous. It was found that SA/M3OG had the highest negative ΔG° value (−9.73 kJ/mol), followed by VA/M3OG (−8.86 kJ/mol), GA/M3OG (−7.57 kJ/mol), PA/M3OG (−6.65 kJ/mol) and *p*HA/M3OG (−6.19 kJ/mol). Obviously, the copigmentation process of methoxylated benzoic acids with M3OG was thermodynamic more favourable than those of hydroxylation benzoic acids, showing that SA and VA were the most efficient cofactors, followed by GA, PA, and *p*HA.

Furthermore, the influence of the temperatures on the copigmentation was also examined. As shown in Fig. 2(a–e), a progressive increase of absorbance (hyperchromic shift) and a shift of the maximum wavelength absorbance toward higher values of the spectrum (bathochromic shift) were observed when the temperatures increased from 10 to 20 °C. But a decrease of hypochromic and hypsochromic shift were seen when the temperatures increased from 20 to 30 °C. The bathochromic and hyperchromic shifts toward higher values observed for the copigmentation complexes could be attributed to the spontaneous processes of the conversions from the reactants to products, as reflected by the

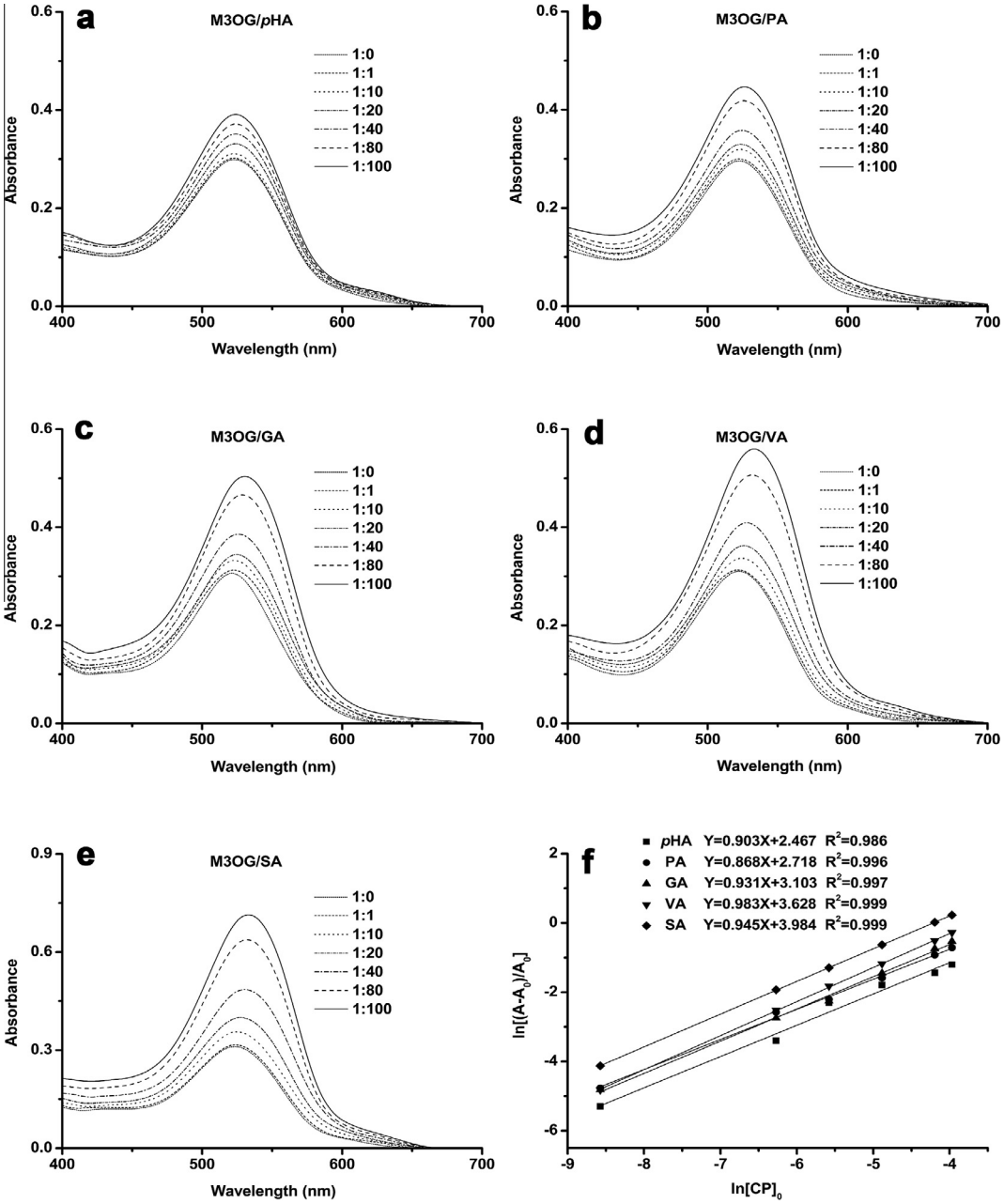

Fig. 1. Visible spectra of free M3OG (1:0) and the pigment/cofactor solutions at different molar ratios (a–e); (f) plots of $\ln[(A - A_0)/A_0]$ *vs* $\ln[CP]_0$ for the copigmentation reactions of M3OG with *p*HA, PA, GA, VA and SA. The intercept was the $\ln K$ value, and the slope was the stoichiometric ratio (n) of the respective copigmentation reaction.

Table 1
Thermodynamic properties of the copigmentaion processes for M3OG with five cofactors.[a]

Cofactor	K ($mol^{-1}L$)	n	ΔG°[b] (kJ mol^{-1})	ΔH°[c] (kJ mol^{-1})	ΔS°[d] (kJ mol^{-1})
*p*HA	12.68	0.904	−6.19	−10.67	−15.29
PA	15.30	0.869	−6.65	−13.49	−23.37
GA	22.39	0.931	−7.57	−16.91	−31.87
VA	37.98	0.983	−8.86	−19.72	−37.06
SA	54.38	0.945	−9.73	−21.09	−38.75

[a] Molar ratio of 1:40, $T = 293$ K.
[b] ΔG° is determined by the Eq. (2): $\Delta G^{\circ} = -RT \times \ln K$.
[c] ΔH° is determined by the slope of the plot of $\ln[(A - A_0)/A_0]$ *vs* $(1/T)$.
[d] ΔS° is determined by the Eq. (3): $\Delta G^{\circ} = \Delta H^{\circ} - T\Delta S^{\circ}$.

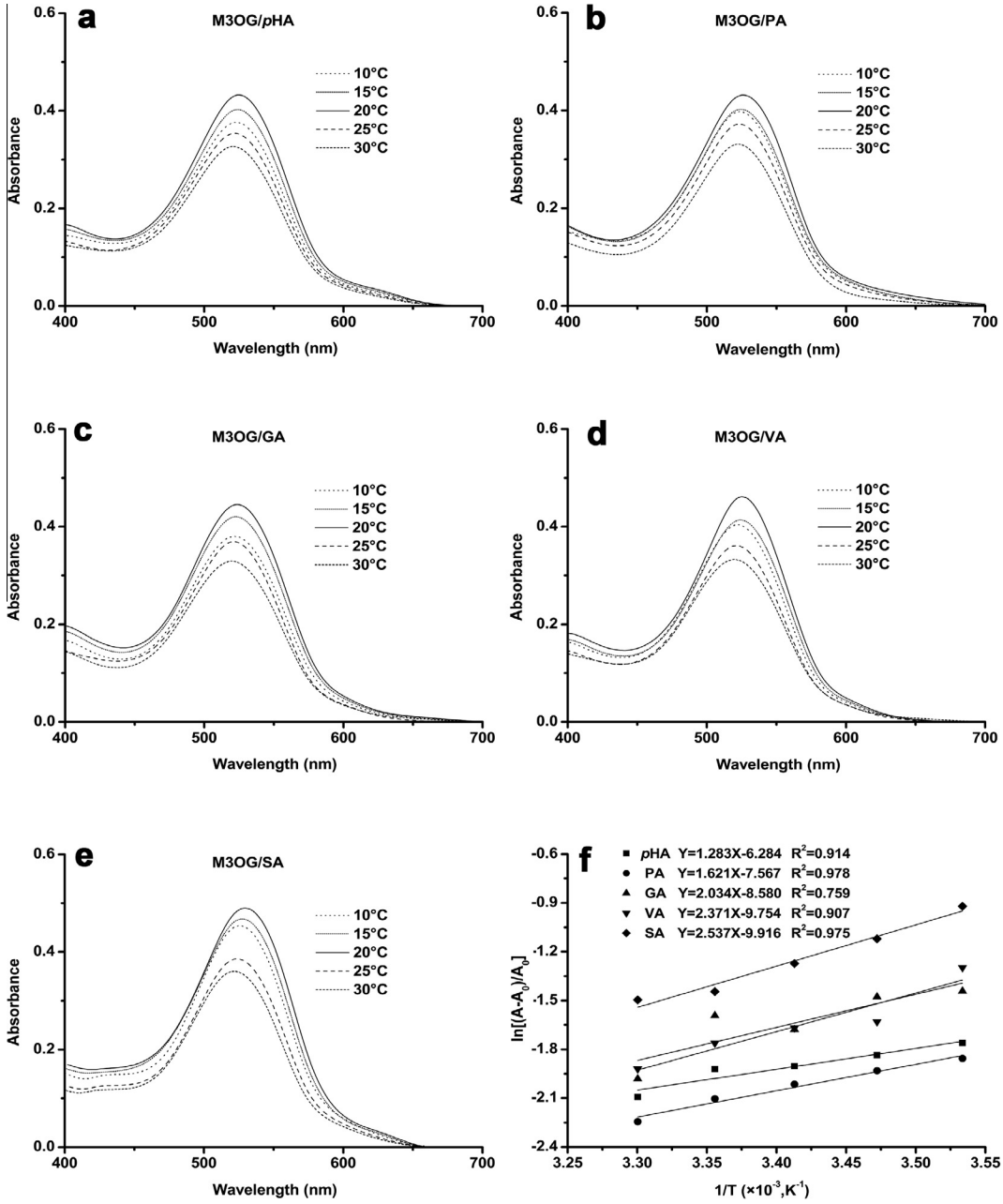

Fig. 2. Visible spectra of the pigment/cofactor solutions (1:40 M ratio) at the temperature ranging from 10 to 30 °C (a–e); (f) plots of $\ln[(A - A_0)/A_0]$ *vs* $(1/T)$ for the copigmentation reactions of M3OG with *p*HA, PA, GA, VA and SA.

negative ΔG° values (Table 1), while their shifts toward lower values meant that the pigment-cofactor copigmentation complex was destroyed and reversed with the further increase of temperature.

The enthalpy variation (ΔH) involved in the copigmentation could be derived by the plot of $\ln[(A - A_0)/A_0]$ *vs* the reciprocal of the temperature ($1/T$), in which ΔH could be determined by the slope of $-\Delta H/R$. The entropy variation (ΔS°) could be calculated from the Gibbs–Helmholtz equation ($\Delta G^\circ = \Delta H^\circ - T\Delta S^\circ$). As seen from Table 1, the ΔG° and ΔH° values were negative for all of these complexes, indicating that theses copigmentations were spontaneous and thermodynamically favored. This finding was consistent with some previous reports (Baranac, Petranovic, & Dimitric-Markovic, 1996; Brouillard et al., 1989; Lambert et al., 2011; Malaj et al., 2013; Markovic et al., 2000; Sun et al., 2010; Teixeira et al., 2013). It was known that the enthalpy change was a measure of the energy barrier that must be overcome by the reacting molecules and related to the strength of the binding (Mercali, Jaeschke, Tessaro, & Marczak, 2013). Therefore, the magnitude of ΔH° suggested that the copigmentation were of low-energy types, which might include the net desolvation which released water molecules from the solvation shells to the bulk solvent by the more hydrophobic cofactor compounds, increasing the van der Waals' force between these molecules and the formation of hydrogen bonds and/or other low-energy interactions. In addition, relatively small change of ΔH° also indicated low affinity of reactants, because of large mole ratio (1:40) of the compounds applied in the experiments. The negative ΔS° values indicated that the copigmentation process was accompanied by entropy loss, and a more stable and orderly structure forms. The negative entropy change suggested that during the association process, both pigments and cofactors underwent reorganization, and the hydrophobic effect did not compensate the loss of rotational and

translational freedom in the anthocyanin and cofactor molecules when they associated (Nave et al., 2012). The interaction between M3OG and SA gave larger negative entropy than either PA (39.7%) or *p*HA (60.5%), indicating that SA gave a more compact complex with a greater degree of order than either PA or *p*HA. Generally, it was widely accepted that the standard enthalpy ΔH° could be considered as a quantitative indicator of the changes in intermolecular bond energies during the binding, while the standard entropy, ΔS°, was most likely a good indicator of the rearrangements undergone by the solvent molecules during the same process (Dangles & Brouillard, 1992). Therefore, we speculated that these reactions were entropy driven with enthalpy contributions.

3.3. Experimental and theoretical investigations of five pigment/cofactor complexes

To better understand the mechanism of copigmentation, theoretical calculations were performed. The experimental and theoretical binding free energies ($\Delta G_{binding}$), relative binding free energies ($\Delta\Delta G_{binding}$) and interaction energies (ΔE) for the five copigmentation complexes were summarized in Table 2. Great differences between the experimental and theoretical $\Delta G_{binding}$ values were observed from the results, which might be associated with the situations of the experiment and the theoretical simulation because the complexes in these two cases experienced different environments. But the stabilities of these complexes had the same tendency, that was, *p*HA/M3OG < PA/M3OG < GA/M3OG < VA/M3OG < SA/M3OG. Compared to other complexes, the most negative $\Delta G_{binding}$ of the SA/M3OG complex revealed that the SA/M3OG complex was thermodynamically more favourable than others. Noticeably, the relative binding free energies ($\Delta\Delta G_{binding}$) obtained at the M062X/6–31G (d, p) level of theory were in qualitative agreement with the experimental results, suggesting that the theoretical method used could provide a useful understanding for the interacting complex. Additionally, the interaction energies (ΔE) for the five complexes showed the same tendency of their stabilities as shown in $\Delta G_{binding}$'s changing, which further confirmed that the SA/M3OG complex is the most stable one.

Table 2
Experimental and theoretical binding free energies ($\Delta G_{binding}$), relative binding free energies ($\Delta\Delta G_{binding}$) and interaction energies (ΔE) for the five copigmentation complexes. (All units are in kcal mol^{-1}.)

Complex	Experimental		Theoretical		
	$\Delta G_{binding}$	$\Delta\Delta G_{binding}$ [a]	$\Delta G_{binding}$	$\Delta\Delta G_{binding}$ [b]	ΔE
*p*HA/M3OG	−1.48	0.85	−1.30	2.81	−17.11
PA/M3OG	−1.59	0.74	−2.08	2.03	−17.94
GA/M3OG	−1.81	0.52	−2.15	1.96	−18.13
VA/M3OG	−2.12	0.21	−3.77	0.34	−20.20
SA/M3OG	−2.33	0.00	−4.11	0.00	−20.39

[a] Experimental values calculated from Table 1 using $\Delta\Delta G_{binding} = RT\ln(K_{SA}/K_{CPx})$.
[b] The binding free energies for the copigmentation complexes relative to SA/M3OG.

Fig. 3 showed the optimized geometries of the five copigmentation complexes. To understand the driving forces for the copigmentation, atoms in molecules (AIM) (Bader, 1991) analysis was used to identify the intermolecular interactions between the pigment and cofactor, which was carried out at the M062X/6–31G(d, p) level of theory. According to the AIM theory, the Laplacian value $\nabla^2\rho$ (i.e., $\nabla^2\rho = \lambda_1 + \lambda_2 + \lambda_3$, where λ_i was an eigenvalue of the Hessian matrix of the electron density ρ) and the electron density ρ could be used to characterize the bond. The positive $\nabla^2\rho$ suggested that the bond belonged to the ionic bond, hydrogen bond (HB) or van der Waals (vdW) interaction. When one of the three eigenvalues were positive and the other two were negative, we denoted it by (3,−1) and called it as the bond critical point (BCP). For BCP,

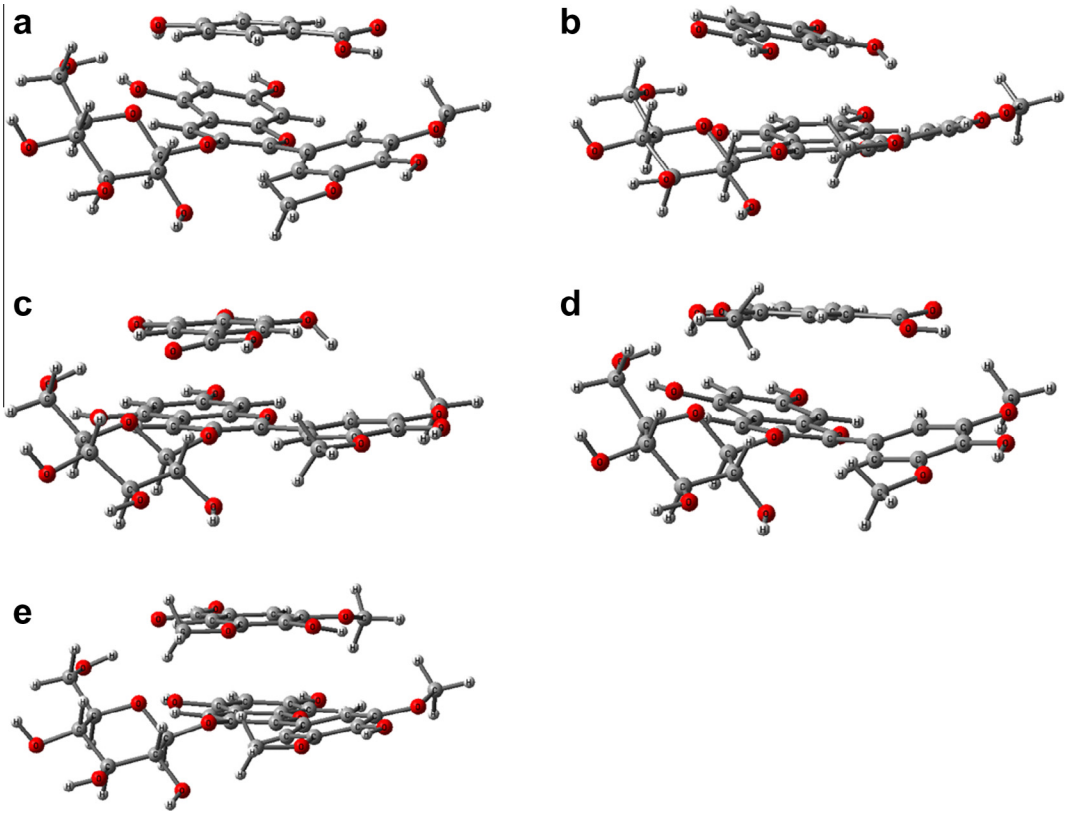

Fig. 3. The optimized geometries of the five copigmentation complexes (a) *p*HA/M3OG; (b) PA/M3OG; (c) GA/M3OG; (d) VA/M3OG; (e) SA/M3OG.

Table 3
The number (n) of the bond critical points (BCP), ring critical points (RCP), cage critical point (CCP) between the cofactor and pigment in the complex and the classification.

Complex	n BCP		n RCP	n CCP
*p*HA/M3OG	10	4 HBs 6 vdWs	17 Close contacts	3 π–π interactions
PA/M3OG	13	6 HBs 7 vdWs	27 Close contacts	7 π–π interactions
GA/M3OG	12	2 HBs 10 vdWs	21 Close contacts	4 π–π interactions
VA/M3OG	13	5 HBs 8 vdWs	21 Close contacts	4 π–π interactions
SA/M3OG	17	3 HBs 14 vdWs	30 Close contacts	7 π–π interactions

three criteria were used in distinguishing the HB (Lipkowski, Grabowski, Robinson, & Leszczynski, 2004), which meant there existed a bond critical point, and the electron density ρ and its Laplacian$\bigtriangledown^2\rho$ should be within the ranges of 0.002–0.035 and 0.024–0.139 a.u., respectively. When the electron density ρ was about 10^{-3} a.u. and its $\bigtriangledown^2\rho$ value was smaller than 0.024 a.u., the interaction between two atoms was usually classified as vdW interaction (Zhou & Qiu, 2009). When one of the three eigenvalues was negative and the other two were positive, it was denoted as (3,+1) and was named as the ring critical point (RCP) which indicated the existence of a ring structure. When the three were all positive, it was denoted as (3,+3) and named as the cage critical point (CCP), indicating the formation of a cage between several rings. With regard to the intermolecular RCPs and CCPs, they might be indicative of the close contact and the π–π interaction, respectively. Both these two types' interactions belonged to the vdW interactions. Therefore, the intermolecular interactions between the pigment and cofactor could be derived. As shown in Table 3, HB and vdW interactions were the main driving forces for the formation of these complexes. The carbonyl *O* atom and OH group in the cofactors tended to form HBs with the anthocyanins, while the vdW interactions raised from the close contacts between two atoms and the π–π interactions between these units with π-aromatic rings. The above statistical data showed that the hydrogen bond and van der Waals interactions contribute to the pigment-cofactor copigmentation.

4. Conclusions

In this work, the copigmentation reactions between the pigment (M3OG) and five cofactors (*p*HA, PA, GA, VA and SA) were investigated. The results showed that the increasing concentration of these cofactors led to an increase of the solutions' absorbance (hyperchromic and bathochromic shifts), because of their strong intermolecular interactions. This was associated with the structures of the cofactors, because the cofactors containing more methoxyl group or hydroxyl groups would interact with M3OG to form more stable complexes, leading to the larger hyperchromic and bathochromic shifts: SA/M3OG > VA/M3OG > GA/M3OG > PA/M3OG > *p*HA/M3OG. Besides, the temperature also affected the copigmentation. At lower temperature, ranging from 10 to 20 °C, the hyperchromic and bathochromic shifts toward higher values were observed, but they were reduced to lower values when the temperature increased from 20 to 30 °C. Theoretical calculations conformed that $\Delta\Delta G_{binding}$ of the five copigmentation complexes showed the tendency in good agreement to the experimental values, indicating that the theoretical method used in this research was reliable in simulating their intermolecular interactions, which were further confirmed by the interaction energies (ΔE). Besides, AIM analysis also suggested that the hydrogen bonds and van der Waals interactions serving as the main driving forces contributing to the pigment-cofactor copigmentation. Therefore, the copigmentation processes between M3OG and the five cofactors were strongly dependent on their concentrations, structures, and the reaction temperatures.

Acknowledgement

The authors gratefully acknowledge the financial support received from National Natural Science Foundation of China (Grant No. 31271926) and China Agriculture Research System for Grape Industry (CARS-30).

Appendix A. Supplementary data

Supplementary data associated with this article can be found, in the online version, at http://dx.doi.org/10.1016/j.foodchem.2014.08.026.

References

Aleixandre-Tudó, J. L., Álvarez, I., Lizama, V., Garćia, M. a. J., Aleixandre, J. L., & Du Toit, W. J. (2013). Impact of caffeic acid addition on phenolic composition of tempranillo wines from different winemaking techniques. *Journal of Agricultural and Food Chemistry, 61*(49), 11900–11912.

Álvarez, I., Aleixandre, J. L., García, M. J., Lizama, V., & Aleixandre-Tudó, J. L. (2008). Effect of the prefermentative addition of copigments on the polyphenolic composition of Tempranillo wines after malolactic fermentation. *European Food Research and Technology, 228*(4), 501–510.

Asen, S., Stewart, R. N., & Norris, K. H. (1972). Co-pigmentation of anthocyanins in plant tissues and its effect on colour. *Phytochemistry, 11*(3), 1139–1144.

Bader, R. F. W. (1991). A quantum theory of molecular structure and its applications. *Chemical Reviews, 91*(5), 893–928.

Baranac, J. M., Petranovic, N. A., & Dimitric-Markovic, J. M. (1996). Spectrophotometric study of anthocyan copigmentation reactions. *Journal of agricultural and food chemistry, 44*(5), 1333–1336.

Bloomfield, D. G., Heatherbell, D. A., & Pour Nikfardjam, M. S. (2003). Effect of p-coumaric acid on the colour in red wine. *Mitteilungen Klosterneuburg, 53*, 195–198.

Boulton, R. (2001). The copigmentation of anthocyanins and its role in the colour of red wine: A critical review. *American Journal of Enology and Viticulture, 52*(2), 67–87.

Brouillard, R., & Dangles, O. (1994). Anthocyanin molecular interactions: the first step in the formation of new pigments during wine aging? *Food Chemistry, 51*(4), 365–371.

Brouillard, R., & Delaporte, B. (1977). Chemistry of anthocyanin pigments. 2. Kinetic and thermodynamic study of proton transfer, hydration, and tautomeric reactions of malvidin 3-glucoside. *Journal of the American Chemical Society, 99*(26), 8461–8468.

Brouillard, R., Mazza, G., Saad, Z., Albrecht-Gary, A. M., & Cheminat, A. (1989). The co-pigmentation reaction of anthocyanins: a microprobe for the structural study of aqueous solutions. *Journal of the American Chemical Society, 111*(7), 2604–2610.

Dangles, O., & Brouillard, R. (1992). Polyphenol interactions. The copigmentation case: thermodynamic data from temperature variation and relaxation kinetics. Medium effect. *Canadian Journal of Chemistry, 70*(8), 2174–2189.

Frisch, M., Trucks, G. W., Schlegel, H. B., Scuseria, G. E., Robb, M. A., Cheeseman, J. R., Scalmani, G., Barone, V., Mennucci, B., Petersson, G. A., Nakatsuji, H., Caricato, M., Li, X., Hratchian, H. P., Izmaylov, A. F., Bloino, J., Zheng, G., Sonnenberg, J. L., Hada, M., Ehara, M., Toyota, K., Fukuda, R., Hasegawa, J., Ishida, M., Nakajima, T., Honda, Y., Kitao, O., Nakai, H., Vreven, T., Montgomery, J. A., Jr., Peralta, J. E., Ogliaro, F., Bearpark, M., Heyd, J. J., Brothers, E., Kudin, K., N.;, Staroverov, V. N., Kobayashi, R., Normand, J., Raghavachari, K., Rendell, A., Burant, J. C., Iyengar, S. S., Tomasi, J., Cossi, M., Rega, N., Millam, N. J., Klene, M., Knox, J. E., Cross, J. B., Bakken, V., Adamo, C., Jaramillo, J., Gomperts, R., Stratmann, R. E., Yazyev, O., Austin, A. J., Cammi, R., Pomelli, C., Ochterski, J. W., Martin, R. L., Morokuma, K., Zakrzewski, V. G., Voth, G. A., Salvador, P., Dannenberg, J. J., Dapprich, S., Daniels, A. D., Farkas, O., Foresman, J. B., Ortiz, J. V., Cioslowski, J., & Fox, D. J. (2009). Gaussian 09, Gaussian. *Inc., Wallingford, CT*.

Goto, T. (1987). Structure stability and colour variation of natural anthocyanins. In *Fortschritte der Chemie organischer Naturstoffe/Progress in the Chemistry of Organic Natural Products* (pp. 113–158). Springer.

He, J., & Giusti, M. M. (2010). Anthocyanins: natural colorants with health-promoting properties. *Annual Review of Food Science and Technology, 1*, 163–187.

Kelebek, H., Selli, S., Canbas, A., & Cabaroglu, T. (2009). HPLC determination of organic acids, sugars, phenolic compositions and antioxidant capacity of orange juice and orange wine made from a Turkish cv. Kozan. *Microchemical Journal, 91*(2), 187–192.

Lambert, S. G., Asenstorfer, R. E., Williamson, N. M., Iland, P. G., & Jones, G. P. (2011). Copigmentation between malvidin-3-glucoside and some wine constituents

and its importance to colour expression in red wine. *Food Chemistry, 125*(1), 106–115.
Lipkowski, P., Grabowski, S. J., Robinson, T. L., & Leszczynski, J. (2004). Properties of the CH···H dihydrogen bond: An ab initio and topological analysis. *The Journal of Physical Chemistry A, 108*(49), 10865–10872.
Malaj, N., De Simone, B. C., Quartarolo, A. D., & Russo, N. (2013). Spectrophotometric study of the copigmentation of malvidin 3-O-glucoside with p-coumaric, vanillic and syringic acids. *Food Chemistry, 141*(4), 3614–3620.
Markovic, D., Petranovic, N. A., & Baranac, J. M. (2000). A spectrophotometric study of the copigmentation of malvin with caffeic and ferulic acids. *Journal of Agricultural and Food Chemistry, 48*(11), 5530–5536.
Mercali, G. D., Jaeschke, D. P., Tessaro, I. C., & Marczak, L. D. (2013). Degradation kinetics of anthocyanins in acerola pulp: comparison between ohmic and conventional heat treatment. *Food Chemistry, 136*(2), 853–857.
Mistry, T. V., Cai, Y., Lilley, T. H., & Haslam, E. (1991). Polyphenol interactions. Part 5. Anthocyanin co-pigmentation. *Journal of the Chemical Society, Perkin Transactions, 2*(8), 1287–1296.
Nave, F., Brás, N. r. F., Cruz, L., Teixeira, N., Mateus, N., Ramos, M. J., et al. (2012). Influence of a flavan-3-ol substituent on the affinity of anthocyanins (pigments) toward vinylcatechin dimers and proanthocyanidins (copigments). *The Journal of Physical Chemistry B, 116*(48), 14089–14099.
Nonier Bourden, M. F., Vivas, N., Absalon, C., Vitry, C., Fouquet, E., & Vivas de Gaulejac, N. (2008). Structural diversity of nucleophilic adducts from flavanols and oak wood aldehydes. *Food Chemistry, 107*(4), 1494–1505.
Qin, Y., Xia, M., Ma, J., Hao, Y., Liu, J., Mou, H., et al. (2009). Anthocyanin supplementation improves serum LDL-and HDL-cholesterol concentrations associated with the inhibition of cholesteryl ester transfer protein in dyslipidemic subjects. *The American Journal Of Clinical Nutrition, 90*(3), 485–492.
Rein, M. (2005). Copigmentation reactions and colour stability of berry anthocyanins. University of Helsinki.
Sancho, R. A. S., & Pastore, G. M. (2012). Evaluation of the effects of anthocyanins in type 2 diabetes. *Food Research International, 46*(1), 378–386.
Santos-Buelga, C., & de Freitas, V. (2009). Influence of phenolics on wine organoleptic properties. In *Wine Chemistry and Biochemistry* (pp. 529–570). Springer.
Schwarz, M., Picazo-Bacete, J. J., Winterhalter, P., & Hermosín-Gutiérrez, I. (2005). Effect of copigments and grape cultivar on the colour of red wines fermented after the addition of copigments. *Journal of Agricultural and Food Chemistry, 53*(21), 8372–8381.
Sousa, A., Araújo, P., Cruz, L., Brás, N. F., Mateus, N., & De Freitas, V. (2014). Evidence for copigmentation interactions between deoxyanthocyanidin derivatives (oaklins) and common copigments in wine model solutions. *Journal of Agricultural and Food Chemistry*. http://dx.doi.org/10.1021/jf404640m.
Sun, J., Cao, X., Bai, w., Liao, X., & Hu, X. (2010). Comparative analyses of copigmentation of cyanidin 3-glucoside and cyanidin 3-sophoroside from red raspberry fruits. *Food Chemistry, 120*(4), 1131–1137.
Teixeira, N., Cruz, L., Bras, N. F., Mateus, N., Ramos, M. J., & de Freitas, V. (2013). Structural features of copigmentation of oenin with different polyphenol copigments. *Journal of Agricultural and Food Chemistry, 61*(28), 6942–6948.
Vauzour, D., Rodriguez-Mateos, A., Corona, G., Oruna-Concha, M. J., & Spencer, J. P. E. (2010). Polyphenols and human health: prevention of disease and mechanisms of action. *Nutrients, 2*(11), 1106–1131.
Zhao, Y., & Truhlar, D. G. (2006). A new local density functional for main-group thermochemistry, transition metal bonding, thermochemical kinetics, and noncovalent interactions. *J. Chem. Phys., 125*(19), 194101.
Zhao, Y., & Truhlar, D. G. (2008). Density functionals with broad applicability in chemistry. *Accounts of Chemical Research, 41*(2), 157–167.
Zhou, P. P., & Qiu, W. Y. (2009). Red-shifted hydrogen bonds and blue-shifted van der Waals contact in the standard Watson–Crick adenine–thymine base pair. *The Journal of Physical Chemistry A, 113*(38), 10306–10320.